

## Spectroscopically Distinct Sites Present in Methyltrioxorhenium Grafted onto Silica–Alumina, and Their Abilities to Initiate Olefin Metathesis

Anthony W. Moses,<sup>†</sup> Christina Raab,<sup>†</sup> Ryan C. Nelson,<sup>†</sup> Heather D. Leifeste,<sup>†</sup>  
Naseem A. Ramsahye,<sup>†</sup> Swarup Chattopadhyay,<sup>†</sup> Juergen Eckert,<sup>‡,§</sup>  
Bradley F. Chmelka,<sup>\*,†</sup> and Susannah L. Scott<sup>\*,†,||</sup>

*Contribution from the Department of Chemical Engineering, Department of Chemistry, and Materials Research Laboratory, University of California, Santa Barbara, California 93106 and the Manuel Lujan, Jr., Neutron Scattering Center, Los Alamos National Laboratory, Los Alamos, New Mexico 87545*

Received April 18, 2007; E-mail: bradc@engineering.ucsb.edu; sscott@engineering.ucsb.edu

**Abstract:** Deposition of  $\text{CH}_3\text{ReO}_3$  onto the surface of dehydrated, amorphous silica–alumina generates a highly active, supported catalyst for the metathesis of olefins. However, silica–alumina with a high (10 wt %) Re loading is no more active than silica–alumina with low (1 wt %) loading, while  $\text{CH}_3\text{ReO}_3$  on silica is completely inactive. Catalysts prepared by grafting  $\text{CH}_3\text{ReO}_3$  on silica–alumina contain two types of spectroscopically distinct sites. The more strongly bound sites are responsible for olefin metathesis activity and are formed preferentially at low Re loadings ( $\leq 1$  wt %). They are created by two Lewis acid/base interactions: (1) the coordination of an oxo ligand to an Al center of the support and (2) interaction of one of the adjacent bridging oxygens (AIOSi) with the Re center. At higher Re loadings (1–10 wt %),  $\text{CH}_3\text{ReO}_3$  also interacts with surface silanols by H-bonding. This gives rise to highly mobile sites, most of which can be observed by  $^{13}\text{C}$  solid-state NMR even without magic-angle spinning. Their formation can be prevented by capping the surface hydroxyl groups with hexamethyldisilazane prior to grafting  $\text{CH}_3\text{ReO}_3$ , resulting in a metathesis catalyst that is more selective, more robust, and more efficient in terms of Re use.

### Introduction

Methyltrioxorhenium ( $\text{CH}_3\text{ReO}_3$ ) deposited on silica–alumina is a catalyst for the metathesis of olefins.<sup>1,2</sup> The silica–alumina must serve as an activator as well as a catalyst support, because solutions of  $\text{CH}_3\text{ReO}_3$  do not catalyze homogeneous olefin metathesis. The amorphous nature of the silica–alumina also appears to be crucial, since crystalline aluminosilicates are much less effective in activating  $\text{CH}_3\text{ReO}_3$ .<sup>3</sup> Recently, we reported experimental evidence for an early suggestion<sup>1</sup> that  $\text{CH}_3\text{ReO}_3$  is formed upon treatment of silica- and silica–alumina-supported perhenates with the promoter  $(\text{CH}_3)_4\text{Sn}$ .<sup>4</sup>

The nature of the interaction between  $\text{CH}_3\text{ReO}_3$  and silica–alumina or aluminosilicates, as well as the mechanism of activation of the resulting supported  $\text{CH}_3\text{ReO}_3$  for olefin metathesis, has been the object of several inquiries. A hydrogen-bonding interaction was proposed for  $\text{CH}_3\text{ReO}_3$  in zeolites,<sup>3,5</sup>

while condensation with the surface hydroxyls was suggested for  $\text{CH}_3\text{ReO}_3$  on silica and silica–alumina.<sup>6</sup> However, solid oxides possess a variety of Lewis and Brønsted acidic and basic centers that can serve as grafting sites for organometallic catalysts. In the presence of such heterogeneity, positive identification of the structures of the sites that become activated in the catalytic reaction is challenging.

Solid-state NMR spectroscopy is a powerful tool for investigating supported organometallic catalysts, because the chemical shift can be highly sensitive to variations in the ligand environment, while the line width provides information about site mobility. Prior to grafting, organometallic complexes can be selectively modified by introduction of NMR-active isotope labels to provide further insights into the nature of the surface species. In this work, we combine solid-state NMR and IR measurements with computational analyses to explore the structures of the major sites formed by grafting  $\text{CH}_3\text{ReO}_3$  onto amorphous silica–alumina, and we establish some of their relationships to the olefin metathesis activity of this material. These insights point to simple modifications in catalyst preparation that lead to higher selectivity, less leaching, and more efficient use of the expensive Re complex.

### Experimental Methods

**Materials.** The silica–alumina, Davicat 3113 (7.6 wt % Al, BET surface area 573  $\text{m}^2/\text{g}$ , pore volume 0.76  $\text{cm}^3/\text{g}$ ), was

<sup>†</sup> Department of Chemical Engineering.

<sup>‡</sup> Materials Research Laboratory.

<sup>§</sup> Los Alamos National Laboratory.

<sup>||</sup> Department of Chemistry.

(1) Herrmann, W. A.; Kuchler, J. G.; Wagner, W.; Felixberger, J. K.; Herdtweck, E. *Angew. Chem., Int. Ed. Engl.* **1988**, *27*, 394–396.

(2) Herrmann, W. A.; Wagner, W.; Flessner, U. N.; Volkhardt, U.; Komber, H. *Angew. Chem., Int. Ed. Engl.* **1991**, *30*, 1636–1638.

(3) Bein, T.; Huber, C.; Moller, K.; Wu, C.-G.; Xu, L. *Chem. Mater.* **1997**, *9*, 2252–2254.

(4) Moses, A. W.; Leifeste, H. D.; Ramsahye, N. A.; Eckert, J.; Scott, S. L. *Catal. Org. React.* **2006**, *115*, 13–22.

(5) Malek, A.; Ozin, G. A. *Adv. Mater.* **1995**, *7*, 160–163.

provided by Grace-Davison (Columbia, MD). The nonporous, fumed silica Aerosil 380 (BET surface area 340 m<sup>2</sup>/g, average particle size 7 nm) was provided by Degussa (Piscataway, NY). For each experiment, the appropriate amount of the oxide support was first heated in a Pyrex reactor at 450 °C at 10 °C/min and then held at 450 °C under dynamic vacuum ( $\leq 10^{-4}$  Torr) for a minimum of 4 h. The solid was subsequently calcined for 12 h under 350 Torr of O<sub>2</sub> at the same temperature to remove hydrocarbon impurities and surface carbonates and then cooled to room temperature under dynamic vacuum. This treatment is sufficient to completely remove adsorbed water even from highly hygroscopic silica–alumina;<sup>7</sup> therefore these supports are referred to as “dehydrated”. They were subsequently handled under an inert atmosphere or vacuum.

Hexamethyldisilazane (HMDS, Aldrich, >99.5%) was subjected to multiple freeze–pump–thaw cycles to remove dissolved gases and then stored under vacuum over P<sub>2</sub>O<sub>5</sub> in a glass reactor. To prepare trimethylsilyl-capped silica–alumina, HMDS was transferred via the vapor phase under reduced pressure onto the dehydrated support until there was no further uptake (as judged by stabilization of the pressure). The reactor was then evacuated, and the solid was heated to 350 °C for 4 h under dynamic vacuum to remove unreacted HMDS, as well as ammonia produced during the silanol reaction. This procedure results in the capping of ca. 80% of the silanol sites, evaluated by quantitative comparison of the <sup>1</sup>H NMR and IR spectra of capped and uncapped silica–aluminas.

CH<sub>3</sub>ReO<sub>3</sub> (Aldrich, >98.0%) was used as received. To resolve signals in solid-state <sup>1</sup>H NMR experiments and to enhance sensitivity in solid-state <sup>13</sup>C NMR experiments, isotopically labeled CD<sub>3</sub>ReO<sub>3</sub> (>99% D) and <sup>13</sup>CH<sub>3</sub>ReO<sub>3</sub> (>99% <sup>13</sup>C) were also prepared from CD<sub>3</sub>SnBu<sub>3</sub> and <sup>13</sup>CH<sub>3</sub>SnBu<sub>3</sub>, respectively, according to literature procedures.<sup>6,8</sup> In all cases, volatile CH<sub>3</sub>ReO<sub>3</sub>/CD<sub>3</sub>ReO<sub>3</sub> was sublimed at room temperature and 10<sup>−4</sup> Torr into an all-glass reactor containing the dehydrated support. Physisorbed material was recovered by subsequent desorption (ca. 12 h) to a liquid N<sub>2</sub> trap at room temperature under vacuum. However, the desorption step was generally omitted for samples with low Re loadings (far below the maximum uptake by chemisorption, ca. 10 wt.% Re on Davicat 3113) and for the silica support (since CH<sub>3</sub>ReO<sub>3</sub> desorbs completely from silica under these conditions). Where noted, desorption from silica–alumina was performed at 80 °C, by heating the material under vacuum and collecting volatile CH<sub>3</sub>ReO<sub>3</sub> in a liquid N<sub>2</sub>-cooled receiving flask. CH<sub>3</sub>ReO<sub>3</sub>-modified silica–alumina is yellow-brown, while CH<sub>3</sub>ReO<sub>3</sub>-modified silica is pale yellow.

**Rhenium Analysis.** Re loadings were determined by quantitative extraction, followed by UV spectrophotometric analysis. Approximately 15 mg of solid material was first weighed precisely in a dry argon atmosphere. Re was extracted quantitatively as perrhenate by stirring overnight in air with 5 mL of 3 M NaOH. Samples were diluted to 25 mL with 3 M H<sub>2</sub>SO<sub>4</sub> and filtered, and their UV spectra were recorded on a Shimadzu UV2401PC spectrophotometer. The Re concentration was

determined at 224 nm, using a calibration curve prepared with NH<sub>4</sub>ReO<sub>4</sub> (Aldrich). Based on three trials, the *relative* standard deviation of the Re analysis was determined to be 4.6%.

**Kinetics and Selectivity of Propene Metathesis.** A precisely weighed amount (10.0 mg) of each catalyst was loaded into a glass batch reactor (volume ca. 120 mL) under Ar, after which the reactor was removed from the glovebox and evacuated. The section of the reactor containing the catalyst was immersed in an ice bath at 0 °C in order to control the rate of the reaction on a readily monitored time scale, as well as to maintain isothermal reaction conditions. Propene was introduced at the desired pressure via a high vacuum manifold. Aliquots of 1.9 mL were expanded at timed intervals into an evacuated septum port separated from the reactor by a stopcock. 50  $\mu$ L samples of the aliquot were removed with a gastight syringe via a septum. Gases were analyzed by FID on a Shimadzu GC 2010 equipped with a 30 m Supelco Alumina Sulfate PLOT capillary column (0.32 mm i.d.), using the peak area of the small propane contaminant present in the propene as an internal standard.

**Infrared Spectroscopy.** The IR experiment was performed in a Pyrex cell equipped with KCl windows affixed with TorrSeal (Varian). Its high-vacuum ground-glass stopcock and joints were lubricated with Apiezon H grease (Varian). A self-supporting pellet of silica–alumina was prepared in air by pressing ca. 25 mg of the solid at 40 kg/cm<sup>2</sup> in a 16 mm stainless steel die. It was then mounted in a Pyrex pellet holder. Sublimation of CH<sub>3</sub>ReO<sub>3</sub> via a vacuum manifold directly onto the silica–alumina pellet in the presence of TorrSeal led to unwanted side reactions of the latter with the organometallic complex. Instead, the pellet was calcined and dehydrated in an all-glass Schlenk tube, exposed to CH<sub>3</sub>ReO<sub>3</sub> by sublimation, and then transferred to the IR cell in a glovebox. IR spectra of the self-supporting pellet were recorded in transmission mode on a Shimadzu PrestigeIR spectrophotometer equipped with a DTGS detector and purged with CO<sub>2</sub>-free dry air from a Balston 75-52 Purge Gas Generator. Background and sample IR spectra were recorded by co-adding 64 scans at a resolution of 4 cm<sup>−1</sup>.

**NMR Spectroscopy.** Solution-state NMR experiments were performed at room temperature on a Bruker AVANCE 200 spectrometer with a 10-mm broadband probehead, operating at 200.1012 MHz for <sup>1</sup>H and 50.3202 MHz for <sup>13</sup>C. Chloroform-*d* (99.8% D) and benzene-*d*<sub>6</sub> (99.5% D) were purchased from Cambridge Isotopes Laboratories, Inc. (Andover, MA).

Solid-state NMR experiments were performed on a Bruker AVANCE 300 NMR spectrometer with a 4-mm broadband MAS probehead operating at 300.1010 MHz for <sup>1</sup>H and 75.4577 MHz for <sup>13</sup>C. This instrument is equipped with a variable temperature unit. The highly air-sensitive samples were packed into zirconia MAS rotors with tightly fitting caps sealed with Viton R O-rings (Wilmad) under an argon atmosphere in a glovebox equipped with O<sub>2</sub> and moisture sensors. Room-temperature MAS spectra were acquired at a spinning rate of 12 kHz. Low-temperature MAS experiments were recorded while the sample was spinning at 8 kHz.

<sup>1</sup>H MAS experiments were performed with a 90° pulse length of 3.7  $\mu$ s, an acquisition time of 25 ms, and a recycle delay of 3 s. <sup>13</sup>C CP-MAS spectra were recorded using a <sup>13</sup>C 90° pulse length of 3.5  $\mu$ s, a contact time of 3 ms, an acquisition time of 21 ms, a recycle delay of 2 s, and two-pulse phase modulation (TPPM) <sup>1</sup>H decoupling using a pulse length of 6.60  $\mu$ s during

- (6) Morris, L. J.; Downs, A. J.; Greene, T. M.; McGrady, G. S.; Herrmann, W. A.; Sirsch, P.; Scherer, W.; Gropen, O. *Organometallics* **2001**, *20*, 2344–2352.
- (7) Hunger, M.; Freude, D.; Pfeifer, H. *J. Chem. Soc., Faraday Trans.* **1991**, *87*, 657–662.
- (8) Herrmann, W. A.; Kuehn, F. E.; Fischer, R. W.; Thiel, W. R.; Romao, C. *C. Inorg. Chem.* **1992**, *31*, 4431–4432.

$^{13}\text{C}$  signal detection.<sup>9</sup> For single-pulse  $^{13}\text{C}$  MAS experiments, a  $^{13}\text{C}$   $90^\circ$  pulse length of  $3.5\ \mu\text{s}$ , an acquisition time of 25 ms, and a recycle delay of 15 s were used.  $^1\text{H}$  and  $^{13}\text{C}$  chemical shifts were referenced to tetramethylsilane. The same experimental conditions were used in two-dimensional (2-D)  $^{13}\text{C}\{^1\text{H}\}$  HETeronuclear chemical shift CORrelation (HETCOR) experiments. For each of the 256  $t_1$  increments, 128 data acquisitions were collected with a 2 s recycle delay. During the detection period  $t_2$ , 1024 points were collected with a dwell time of  $20\ \mu\text{s}$ . In Figure 3 and Supplementary Figures S2 and S3, the outer contour levels are drawn at 45% of the maximum intensity. No additional correlations were found using lower 2-D threshold levels. The same experimental settings were used for NMR spectra recorded sequentially under MAS/static conditions or at room temperature/ $-100\ ^\circ\text{C}$ . However, in low-temperature experiments, dry  $\text{N}_2$  was used as both the spinning and bearing gas, instead of air.

### Computational Methods

Computations were performed on the VRANA-5 and VRANA-8 clusters at the Center for Molecular Modeling of the National Institute of Chemistry (Ljubljana, Slovenia), as well as Linux workstations with dual Intel Xeon processors using the DFT implementation in the Gaussian03 code, revision C.02.<sup>10</sup> The B3PW91 density functional was used, with a mixed basis set for the orbitals. A fully uncontracted basis set from LANL2DZ was used for the valence electrons of Re,<sup>11</sup> augmented by two  $f$  functions ( $\zeta = 1.14$  and  $0.40$ ) in the full optimization. Re core electrons were treated by the Hay–Wadt relativistic effective core potential (ECP) given by the standard LANL2 parameter set (electron–electron and nucleus–electron). For geometry optimization of the hydrogen-bonded models in Scheme 1, the 6-31+G\*\* basis set was used to describe the rest of the system.

**Calculation of NMR Chemical Shifts.** Proton and  $^{13}\text{C}$  NMR shieldings for computational models of the grafted  $\text{CH}_3\text{ReO}_3$  sites were calculated following a literature method,<sup>12,13</sup> using the 6-311+G(2d, p) basis set for all atoms other than Re and the gauge-independent atomic orbital (GIAO) method. Calculated  $^1\text{H}$  and  $^{13}\text{C}$  shielding values were averaged for chemically equivalent atoms and then converted to NMR chemical shifts via calibration curves constructed from a select set of molecular organorhenium(VII) compounds. In addition to  $\text{CH}_3\text{-ReO}_3$ ,  $[(\text{Me}_3\text{CCH}_2)_2\text{PhReO}_2]$  and  $[\text{Me}_3\text{CCH}_2\text{ReO}_2(=\text{CHC}(\text{CH}_3)_3)]$  were chosen to calibrate the calculated shieldings, based on their Re(VII) formal oxidation state, the availability of crystallographically determined atomic coordinates, and well-documented  $^1\text{H}$  and  $^{13}\text{C}$  NMR chemical shift data.<sup>14</sup> The structures of the calibration compounds were first subjected to geometry optimization, using the 6-31G\* basis set for all atoms other than Re.<sup>15,16</sup> NMR chemical shielding values for the calibration compounds were calculated using the method and basis set described above, with one exception: solvent effects on NMR chemical

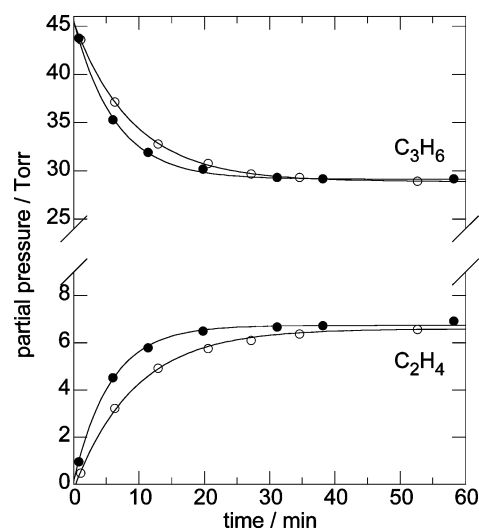


**Figure 1.** Kinetics of propene metathesis (top: disappearance of  $\text{C}_3\text{H}_6$ ; bottom: appearance of  $\text{C}_2\text{H}_4$ ) in a constant-volume batch reactor containing 10.0 mg of  $\text{CH}_3\text{ReO}_3/\text{silica-alumina}$  with 1.0 wt % Re (●) and 10 wt % Re (○), at  $0\ ^\circ\text{C}$ . Solid lines are nonlinear least-squares curve fits to the integrated first-order rate equation.

shifts were included using the polarizable continuum model (PCM). Values are summarized in Tables S1 and S2.

The correlations between calculated NMR shieldings ( $^1\text{H}$ ,  $^{13}\text{C}$ ) and observed isotropic chemical shifts are linear (Figure S1). The maximum  $^1\text{H}$  NMR chemical shift deviation is 0.54 ppm, with an average deviation of 0.35 ppm; the maximum  $^{13}\text{C}$  NMR chemical shift deviation is 4.4 ppm, with an average deviation of 2.1 ppm.

### Results and Discussion

The maximum amount of  $\text{CH}_3\text{ReO}_3$  that is strongly adsorbed by dehydrated Davicat 3113 silica–alumina (i.e., the amount that resists desorption during several hours of evacuation at  $10^{-4}$  Torr and room temperature) corresponds to  $(10 \pm 1)$  wt % Re. Materials with higher Re loadings are unstable, and the excess  $\text{CH}_3\text{ReO}_3$  desorbs rapidly upon evacuation of the reactor. These results suggest that specific grafting sites are responsible for the adsorption of  $\text{CH}_3\text{ReO}_3$  at loadings up to 10 wt % Re.

**Olefin Metathesis Activity and Selectivity.** Dehydrated silica–aluminas with a wide range of  $\text{CH}_3\text{ReO}_3$  loadings (0.1–10 wt % Re) catalyze the self-metathesis of propene. The catalytic activities of two samples, one containing 10 wt % Re and the other containing 1.0 wt % Re, were directly compared under identical reaction conditions ( $0\ ^\circ\text{C}$ , 45 Torr of  $\text{C}_3\text{H}_6$ , 10.0 mg of catalyst). Their kinetic profiles and their corresponding nonlinear first-order curve fits are shown in Figure 1. After 1 h, the partial pressure of ethene and 2-butene isomers formed (13 Torr in total) is slightly lower than the observed decrease in propene partial pressure (16 Torr), due to the well-known adsorption of propene on the silica–alumina surface.<sup>17</sup>

Unexpectedly, the catalyst containing 10 wt % Re was found to be slightly less active for the metathesis of propene ( $k_{\text{obs}} = 0.11\ \text{min}^{-1}$ ) than the catalyst containing 10 times less Re ( $k_{\text{obs}} = 0.18\ \text{s}^{-1}$ ). For the catalyst containing 10 wt % Re on silica–alumina, no olefins other than the expected metathesis products (ethene, *trans*- and *cis*-2-butene) were detected by GC after equilibrium was attained, in ca. 1 h. However, in the same reaction time, the catalyst containing only 1.0 wt % Re on

- (9) Bennett, A. E.; Rienstra, C. M.; Auger, M.; Lakshmi, K. V.; Griffin, R. G. *J. Chem. Phys.* **1995**, *103*, 6951–6958.  
 (10) Frisch, M. J., et al. *Gaussian 03*, revision C.02; Gaussian, Inc.: Wallingford, CT, 2004.  
 (11) Pietsch, M. A.; Russo, T. V.; Murphy, R. B.; Martin, R. L.; Rappe, A. K. *Organometallics* **1998**, *17*, 2716–2719.  
 (12) Forsyth, D. A.; Sebag, A. B. *J. Am. Chem. Soc.* **1997**, *119*, 9483–9494.  
 (13) White, R. E.; Hanusa, T. P. *Organometallics* **2006**, *25*, 5621–5630.  
 (14) Cai, S.; Hoffman, D. M.; Wierda, D. A. *Organometallics* **1996**, *15*, 1023–1032.  
 (15) Unreasonable NMR chemical shifts were obtained when the crystallographically determined atomic coordinates were used without geometry optimization. Comparison of the X-ray crystallographically characterized structures with the geometry-optimized structures revealed that most of the structural differences are in the C–H bond distances. The positions of the heavy atoms are affected to a very small extent by the geometry optimization.  
 (16) Schmidt, J.; Hoffmann, A.; Spiess, H. W.; Sebastiani, D. *J. Phys. Chem. B* **2006**, *110*, 23204–23210.

- (17) MacIver, D. S.; Zabor, R. C.; Emmett, P. H. *J. Phys. Chem.* **1959**, *63*, 484–489.



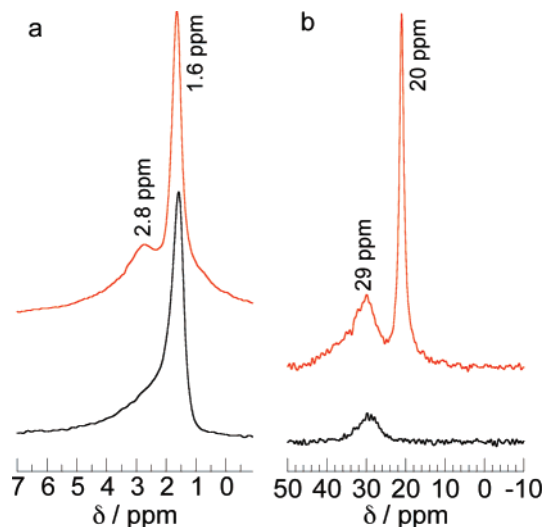


**Figure 2.** Solid-state NMR spectra of  $^{13}\text{CH}_3\text{ReO}_3$  adsorbed onto dehydrated silica–alumina, at two different loadings, 0.4 wt % Re (black) and 10 wt % Re (red): (a) single-pulse  $^1\text{H}$  MAS NMR spectra; (b)  $^{13}\text{C}$  CP-MAS NMR spectra, all acquired at room temperature using an MAS spinning rate of 12 kHz.

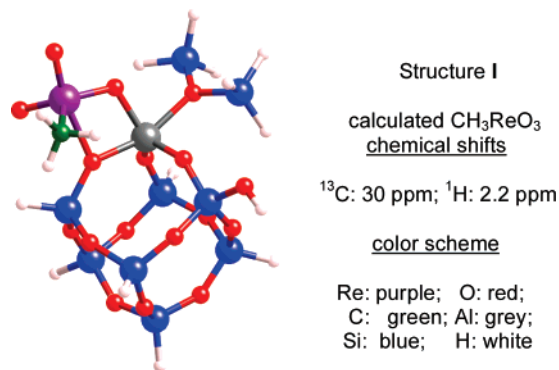
silica–alumina did produce trace amounts of side products, including 1-butene and higher olefins. These products are typical of the olefin isomerization and oligomerization reactions that are catalyzed by the acidic hydroxyl groups of silica–alumina.<sup>18</sup> At longer reaction times, their formation eventually perturbs the equilibrium distribution of olefins arising from propene self-metathesis.

These results suggest that (1) different grafted  $\text{CH}_3\text{ReO}_3$  sites exist with different activities and (2) the first-deposited  $\text{CH}_3\text{ReO}_3$  sites, formed preferentially at low Re loadings on silica–alumina, are responsible for metathesis activity, while later-deposited  $\text{CH}_3\text{ReO}_3$  influences selectivity (by blocking the acidic silanol sites on the silica–alumina surface responsible for side reactions, as shown below).

**Deposition of  $\text{CH}_3\text{ReO}_3$  at Low Loading on Silica–Alumina.** Recently, we reported spectroscopic and computational evidence for the most energetically favored interaction of  $\text{CH}_3\text{ReO}_3$  with the surface of an amorphous, dehydrated silica–alumina.<sup>19</sup> For samples with low Re loadings ( $\leq 1$  wt %), the  $^1\text{H}$  MAS NMR spectrum is dominated by a signal from the surface silanol protons of the silica–alumina support at 1.6 ppm,<sup>20,21</sup> as shown here for a sample with 0.4 wt % Re in Figure 2a (bottom). A quantitative  $^1\text{H}$  MAS NMR experiment demonstrated that silanols are not consumed in this grafting process. At low  $\text{CH}_3\text{ReO}_3$  loadings ( $< 1$  wt % Re), the methyl signal generally cannot be resolved in the 1-D  $^1\text{H}$  NMR spectrum. However, at higher loadings (e.g., 10 wt % Re), the  $^1\text{H}$  MAS spectrum yields a partly resolved signal at 2.8 ppm (Figure 2a (top)), which has been assigned to the methyl protons of grafted  $\text{CH}_3\text{ReO}_3$  according to its correlation to the  $^{13}\text{C}$  signal of the same site in a 2-D  $^{13}\text{C}\{^1\text{H}\}$  HETCOR experiment.<sup>19</sup> For comparison, the isotropic  $^1\text{H}$  chemical shift of  $\text{CH}_3\text{ReO}_3$  in  $\text{CDCl}_3$  is 2.64 ppm.

Silica–alumina containing a low loading of grafted  $\text{CH}_3\text{ReO}_3$  ( $\leq 1$  wt % Re) exhibits a single, broad  $^{13}\text{C}$  CP-MAS peak with a chemical shift of 29 ppm (fwhm 6.10 ppm/460 Hz), Figure 2b (bottom). For comparison, the  $^{13}\text{C}$  chemical shift of  $\text{CH}_3\text{ReO}_3$  in  $\text{CDCl}_3$  is 19.6 ppm, while the  $^{13}\text{C}$  CP-MAS spectrum of polycrystalline  $\text{CH}_3\text{ReO}_3$  shows a complex line shape with maximum intensity at 34 ppm. The simple line shape in Figure 2b (bottom) suggests that the organorhenium complex is indeed molecularly dispersed on the silica–alumina support.

According to our recent DFT study, the most favorable grafting process involves two synergistic Lewis acid–base interactions.<sup>19</sup> One oxo ligand of  $\text{CH}_3\text{ReO}_3$  binds to a Lewis acidic Al site of the silica–alumina surface, while a neighboring framework oxygen (AlOSi) binds to Re. This is depicted in structure I, with an aluminosilsequioxane monosilanol cube



representing the functional group (Lewis acid and base, Brønsted acid) sites present on the surface of amorphous silica–alumina. The aluminum corner is capped with a neutral siloxane ligand to model the dominant coordination environment of the distorted, four-coordinate Al sites in dehydrated silica–alumina.<sup>22</sup> Interaction of  $\text{CH}_3\text{ReO}_3$  with the cube model is accompanied by an increase in the coordination number of the aluminum center.

The calculated  $^{13}\text{C}$  and  $^1\text{H}$  NMR isotropic chemical shifts for structure I, 30 and 2.2 ppm, respectively, agree reasonably well with the observed chemical shifts, at 29 and 2.8 ppm. Evidence for five-coordinate Al in the silica–alumina sites interacting with  $\text{CH}_3\text{ReO}_3$  was found by curve-fitting EXAFS data recorded at the Re  $L_{\text{III}}$ -edge.<sup>19</sup> The broad  $^{13}\text{C}$  CP-MAS NMR signal at 29 ppm that appears at low  $\text{CH}_3\text{ReO}_3$  loadings on silica–alumina is therefore assigned to surface analogues of structure I.

**Deposition of Higher Loadings of  $\text{CH}_3\text{ReO}_3$  on Silica–Alumina.** The  $^1\text{H}$  MAS spectrum of silica–alumina containing 10 wt % Re as  $\text{CH}_3\text{ReO}_3$  is shown in Figure 2a (top). The peak for the methyl protons, at 2.8 ppm, is clearly resolved and more intense relative to the signal at 1.6 ppm for the surface hydroxyl protons compared to the sample with only 0.4 wt % Re, and consistent with the higher Re loading. In contrast, the  $^{13}\text{C}$  CP-MAS spectrum is qualitatively different. Whereas at low loading (0.4 wt % Re), only one relatively broad signal is present at 29 ppm, a narrower signal is also evident at 20 ppm at higher loading (10 wt % Re), Figure 2b (top). The latter spectrum demonstrates the existence of at least two chemically distinct  $^{13}\text{C}$  environments for grafted  $\text{CH}_3\text{ReO}_3$  at the higher Re loading.

(18) Pater, J. P. G.; Jacobs, P. A.; Martens, J. A. *J. Catal.* **1999**, *184*, 262–267.

(19) Moses, A. W.; Ramsahye, N. A.; Raab, C.; Leifeste, H. D.; Chattopadhyay, S.; Chmelka, B. F.; Eckert, J.; Scott, S. L. *Organometallics* **2006**, *25*, 2157–2165.

(20) Hunger, M.; Freude, D.; Pfeifer, H.; Bremer, H.; Jank, M.; Wendlandt, K.-P. *Chem. Phys. Lett.* **1983**, *100*, 29–33.

(21) Dorémieux-Morin, C.; Heeribout, L.; Dumousseaux, C.; Fraissard, J.; Hommel, H.; Legrand, A. P. *J. Am. Chem. Soc.* **1996**, *118*, 13040–13045.

(22) Omegna, A.; van Bokhoven, J. A.; Prins, R. *J. Phys. Chem. B* **2003**, *107*, 8854–8860.

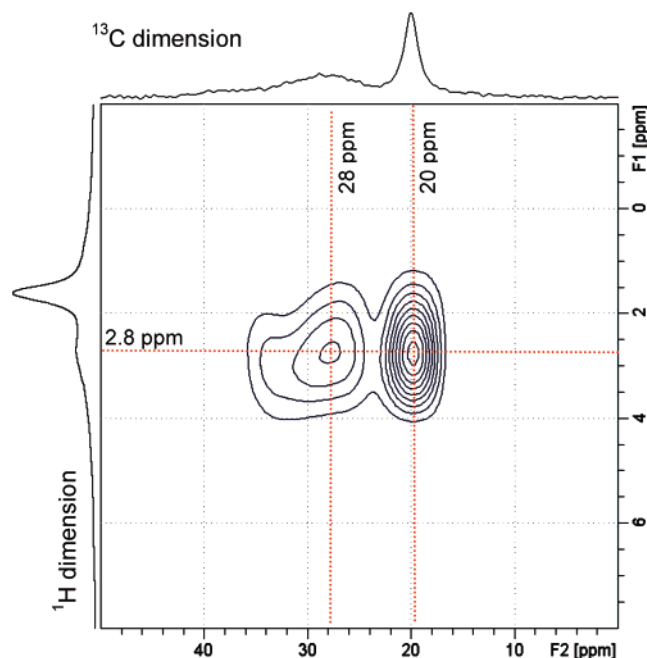


**Figure 3.** Two-dimensional  $^{13}\text{C}\{^1\text{H}\}$  HETCOR MAS NMR spectrum for silica–alumina modified with  $^{13}\text{CH}_3\text{ReO}_3$  (10 wt % Re), recorded at room temperature with a mixing time of 3 ms and an MAS spinning rate of 12 kHz. The corresponding 1-D  $^{13}\text{C}$  CP-MAS and single-pulse  $^1\text{H}$  MAS NMR spectra are plotted along their respective axes.

The chemical shift of the  $^{13}\text{C}$  CP-MAS signal at 20 ppm resembles that of  $\text{CH}_3\text{ReO}_3$  in  $\text{CDCl}_3$  at 19.6 ppm. The relatively narrow line width (fwhm 1.26 ppm/95 Hz) indicates that these grafted sites experience more uniform environments (due to either higher mobility or greater local order) than the sites represented by the broad peak centered at 29 ppm (fwhm 6.10 ppm/460 Hz). Moreover, the narrow signal persists even after room-temperature evacuation of the solid for several hours at  $\leq 10^{-4}$  Torr, establishing that it cannot be attributed to physisorbed  $\text{CH}_3\text{ReO}_3$ . Narrow  $^{13}\text{C}$  CP-MAS NMR lines are unusual for supported organometallic complexes, which typically experience greatly reduced mobility when covalently bound to heterogeneous oxide surfaces, and thus exhibit broad solid-state NMR peaks.<sup>23</sup> For example, the sites that give rise to the broad  $^{13}\text{C}$  signal at ca. 29 ppm, attributed to  $\text{CH}_3\text{ReO}_3$  immobilized by two-point grafting onto adjacent Lewis acid/base sites, appear to be just such heterogeneous, low-mobility sites.

The integrated intensities of the correlated signals observed in solid-state 2D NMR  $^{13}\text{C}\{^1\text{H}\}$  HETCOR experiments depend on the populations of  $^1\text{H}$ – $^{13}\text{C}$  spin pairs and the strengths of their associated dipole–dipole couplings. As shown in Figure 3, the 2-D  $^{13}\text{C}\{^1\text{H}\}$  HETCOR spectrum of  $\text{CH}_3\text{ReO}_3/\text{silica}$ –alumina (10 wt % Re) shows intensity correlations for both of the  $^{13}\text{C}$  methyl signals at 20 and 28 ppm with the broad  $^1\text{H}$  signals centered at 2.8 ppm.<sup>24</sup> Thus the methyl ligand is intact at both grafted sites, and the mobility of each site is low enough to produce efficient dipole–dipole couplings. No correlations were detected between either of the  $^{13}\text{C}$  signals and the terminal, non-hydrogen-bonded silanol  $^1\text{H}$  signal at 1.6 ppm, even when the temperature was lowered to  $-100$  °C and the contact time was increased from 3 to 12 ms to probe weaker couplings

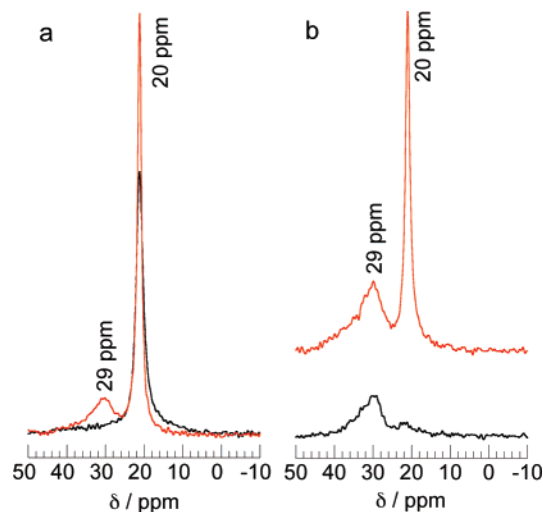


**Figure 4.** Room-temperature  $^{13}\text{C}$  NMR spectra for  $^{13}\text{CH}_3\text{ReO}_3$  adsorbed onto dehydrated silica–alumina. (a) Single-pulse  $^{13}\text{C}$  spectra were acquired consecutively for the same sample (6.5 wt % Re) with the same number of scans, under both MAS (12 kHz, red) and static conditions (black); (b)  $^{13}\text{C}$  CP-MAS spectra (12 kHz) acquired for the same material before (10 wt % Re, red) and after (6 wt % Re, black) desorption of volatiles at 80 °C for 6 h.

(Figure S2). Consequently, both grafted sites are relatively distant from these silanols ( $>1$  nm).

The dynamics of the more mobile of the two types of grafted species were probed with static (non-MAS) solid-state NMR experiments. The room-temperature single-pulse  $^{13}\text{C}$  NMR spectra of a sample of  $^{13}\text{CH}_3\text{ReO}_3$  on silica–alumina (6.5 wt % Re), acquired under both MAS and static conditions, are compared in Figure 4a. Whereas chemical shift anisotropy and dipole–dipole interactions are averaged by rapid molecular motion or under fast MAS conditions, they generally lead to broad spectral lines in solid samples under static conditions. Consequently, without MAS the  $^{13}\text{C}$  signals associated with grafted organometallic species are often undetectable. As expected, the peak at 29 ppm is broadened into the spectral baseline without MAS, confirming that the species responsible for this signal possess low mobility. The line width of the peak at 20 ppm increases slightly to 2.65 ppm fwhm (200 Hz), compared to 2.26 ppm (171 Hz) with 12 kHz MAS, but remains surprisingly narrow.

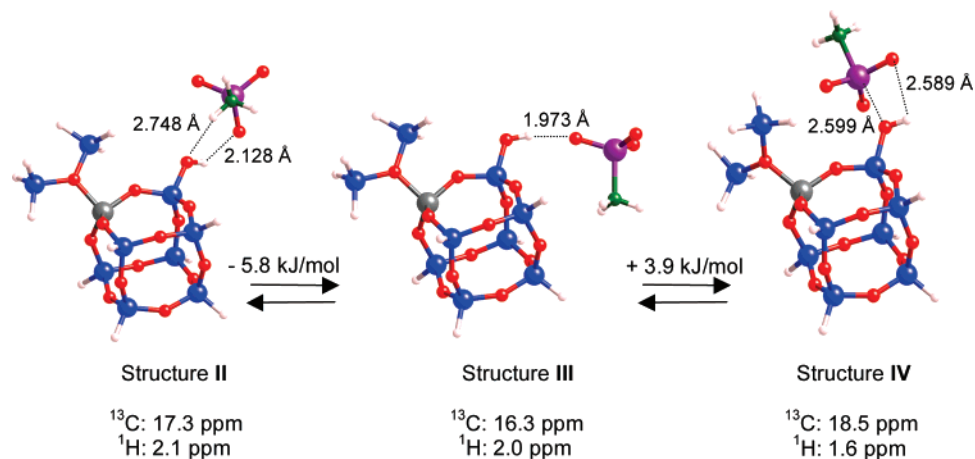
This finding of high mobility was confirmed with low-temperature NMR measurements, in which reduced molecular mobility results in diminished motional averaging of chemical shift anisotropy and dipole–dipole interactions. Lower mobility is typically manifested by greatly increased line widths. Nevertheless, the  $^{13}\text{C}$  signal at 20 ppm is still visible, albeit broadened (fwhm 13 ppm/1000 Hz), at  $-100$  °C under static (non-MAS) conditions, Figure 5. Thus some mobility of grafted  $\text{CH}_3\text{ReO}_3$  persists even at  $-100$  °C.

Evacuation at elevated temperatures results in partial desorption of  $\text{CH}_3\text{ReO}_3$  from the silica–alumina surface.  $^{13}\text{C}$  CP-MAS NMR spectra recorded before and after heating a sample initially containing 10 wt % Re at 80 °C and  $10^{-4}$  Torr for 6 h are compared in Figure 4b. Prior to heating, the relative areas of the peaks at 29 and 20 ppm were ca. 2:1 (Figure 4b, top). Upon

(23) Fischer, H. E.; King, S. A.; Bronnimann, C. E.; Schwartz, J. *Langmuir* **1993**, *9*, 391–393.

(24) Only one  $^1\text{H}$  signal was resolved, even at high loading (10 wt % Re), presumably because of the smaller chemical shift range for  $^1\text{H}$  compared to  $^{13}\text{C}$ .

**Scheme 1.** DFT-Calculated Structures and Energy Differences for  $\text{CH}_3\text{ReO}_3$  Interacting by H-Bonding with an Aluminosilsesquioxane Monosilanol Cube (Representing the Silica–Alumina Surface)<sup>a</sup>



<sup>a</sup> Calculated chemical shifts for the grafted  $\text{CH}_3\text{ReO}_3$  fragment are shown. Color scheme: Re (purple), Al (gray), Si (blue), O (red), C (green), H (white).

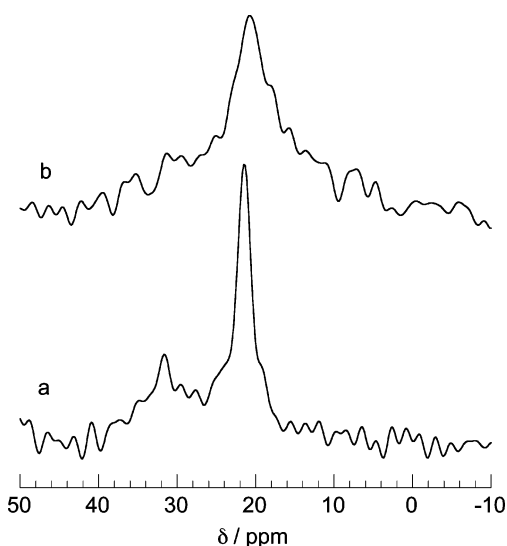


**Figure 5.**  $^{13}\text{C}$  CP NMR spectra for  $\text{CH}_3\text{ReO}_3$  grafted onto dehydrated silica–alumina (10 wt % Re). Both spectra were recorded at  $-100\text{ }^\circ\text{C}$ , (a) with 8 kHz MAS and (b) without spinning.

thermal treatment, the  $^{13}\text{C}$  signal at 20 ppm disappeared, consistent with weaker binding of the more mobile grafted  $\text{CH}_3\text{ReO}_3$  sites (Figure 4b, bottom). At the same time, the Re content of the solid decreased to 6 wt % Re, implying desorption of some of the organometallic complex from the silica–alumina.

**Computational Investigation of Mobile, Grafted  $\text{CH}_3\text{ReO}_3$  on Silica–Alumina.** Highly mobile supported organic and organometallic molecules with narrow MAS NMR spectral lines have been reported in cases where adsorption occurs via weak electrostatic interactions or by ion-pair formation.<sup>25–27</sup> The possible protonation of  $\text{CH}_3\text{ReO}_3$  was investigated by using DFT and the same aluminosilsesquioxane monosilanol cube model used in structure **I** to represent the silica–alumina surface. The cation  $[\text{CH}_3\text{Re}(\text{O})_2(\text{OH})]^+$  was found to be highly energetic, and the proton moved spontaneously back to the aluminosilsesquioxane monosilanolate anion, thus ruling out the formation of stable ion pairs.

$\text{CH}_3\text{ReO}_3$  has been suggested to interact with strongly acidic bridging hydroxyl groups in zeolites via H-bonding, on the basis of the close resemblance in the EXAFS spectra of polycrystalline  $\text{CH}_3\text{ReO}_3$  before and after its adsorption on zeolite HY, as well as a red shift in the frequency of a mode assigned to  $\nu(\text{Re}=\text{O})$ .<sup>3,5</sup> Since silica–alumina is also strongly Brønsted acidic,<sup>28</sup> although lacking bridging hydroxyls,<sup>22,28,29</sup> we considered hydrogen-bonding interactions between  $\text{CH}_3\text{ReO}_3$  and the terminal surface hydroxyl groups as a means of creating highly mobile sites. It has been proposed that some of the terminal silanols of the silica–alumina surface acquire strong Brønsted acidity by virtue of possessing one or more Al neighbors.<sup>28</sup> Three model structures were calculated for the interaction of  $\text{CH}_3\text{ReO}_3$  with the silanol of the aluminosilsesquioxane monosilanol cube, Scheme 1. Structure **III** has a single H-bond between the terminal silanol and an oxo ligand of  $\text{CH}_3\text{ReO}_3$ , with a calculated H-bond energy of 17 kJ/mol. In structure **II**, there is a second H-bond between a methyl proton and the silanol oxygen, similar to those calculated for a dimer of  $\text{CH}_3\text{ReO}_3$ , as well as for a  $\text{CH}_3\text{ReO}_3$ –methanol adduct.<sup>30</sup> H-Bonding involving the methyl protons is also implied in the differing C–H bond lengths observed in the structure of polycrystalline  $\text{CH}_3\text{ReO}_3$  obtained by single-crystal neutron diffraction.<sup>31</sup> In structure **IV**, there is an additional Lewis acid/base interaction between Re and the silanol oxygen, analogous to that proposed on the basis of the  $^{17}\text{O}$  NMR spectrum of  $\text{CH}_3\text{ReO}_3$  in methanol<sup>32</sup> and calculated for a related methanol adduct of  $\text{CH}_3\text{ReO}_3$ .<sup>30</sup> The small energy differences between the model structures in Scheme 1 and the inherent accuracy of the DFT calculations ( $\pm$  several kJ/mol)<sup>11</sup> make it likely that all three structures coexist on the silica–alumina surface and that they interconvert readily.

The calculated isotropic  $^{13}\text{C}$  chemical shifts associated with the grafted  $\text{CH}_3\text{ReO}_3$  sites in each of the structures **II**, **III**, and **IV** (17.3, 16.3, and 18.5 ppm, respectively) all lie close to the

- (25) Scott, S. L.; Dufour, P.; Santini, C. C.; Basset, J.-M. *J. Chem. Soc., Chem. Commun.* **1994**, 2011–2012.  
 (26) Scott, S. L.; Spakowicz, M.; Mills, A.; Santini, C. C. *J. Am. Chem. Soc.* **1998**, *120*, 1883–1890.  
 (27) Pan, V. H.; Tao, T.; Zhou, J.-W.; Maciel, G. E. *J. Phys. Chem. B* **1999**, *103*, 6930–6943.

- (28) Crépeau, G.; Montouillet, V.; Vimont, A.; Mariey, L.; Cseri, T.; Mauge, F. *J. Phys. Chem. B* **2006**, *110*, 15172–15185.  
 (29) Dorémieux-Morin, C.; Martin, C.; Brégault, J.-M.; Fraissard, J. *Appl. Catal.* **1991**, *77*, 149–161.  
 (30) Vaz, P. D.; Ribeiro-Claro, P. J. A. *Eur. J. Inorg. Chem.* **2005**, 1836–1840.  
 (31) Herrmann, W. A.; Scherer, W.; Fischer, R. W.; Blümel, J.; Kleine, M.; Gruehn, R.; Mink, J.; Boysen, H.; Wilson, C. C.; Ibberson, R. M.; Bachmann, L.; Mattner, M. *J. Am. Chem. Soc.* **1995**, *117*, 3231–3242.



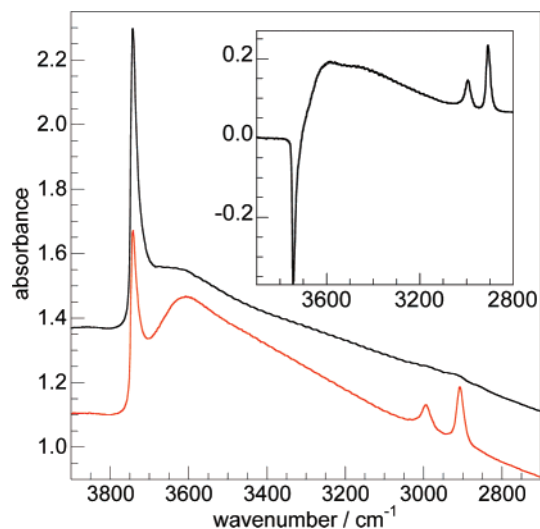


**Figure 6.** IR spectra of dehydrated silica–alumina before (black) and after (red) adsorbing  $\text{CH}_3\text{ReO}_3$  (ca. 10 wt % Re), and the difference spectrum (inset).

experimentally observed  $^{13}\text{C}$  chemical shift for the relatively mobile  $\text{CH}_3\text{ReO}_3$  sites (20 ppm), as well as  $\text{CH}_3\text{ReO}_3$  in  $\text{CDCl}_3$  (19.6 ppm). High mobility in structure **III** can arise by rotation of the  $[\text{CH}_3\text{ReO}_2]$  fragment about the  $\text{Re}-\text{O}-\text{H}-\text{O}$  axis, as well as rotation of the  $[\text{CH}_3\text{ReO}_3\text{H}]$  fragment about the  $\text{Si}-\text{O}$  axis. In addition,  $\text{CH}_3\text{ReO}_3$  may interchange H-bonded and non-H-bonded oxo ligands via a hopping mechanism. Rapid interconversion between structures **II**, **III**, and **IV**, as well as migration between silanol sites, may also contribute to the narrowness of the  $^{13}\text{C}$  NMR signal.

**Evidence for H-Bonded  $\text{CH}_3\text{ReO}_3$  on Silica–Alumina.** The lower rate of side reactions over the catalyst with the higher Re loading is consistent with blocking of the acidic hydroxyl sites by adsorption of  $\text{CH}_3\text{ReO}_3$ , as modeled by structures **II–IV**. The IR spectra of a self-supporting pellet of dehydrated silica–alumina, recorded before and after deposition of  $\text{CH}_3\text{ReO}_3$ , provide direct evidence for this hydrogen-bonding interaction. Grafting results in a decrease in the intensity of the  $\nu(\text{SiO}-\text{H})$  mode at  $3747\text{ cm}^{-1}$  attributed to noninteracting surface silanols and the appearance of a broad, red-shifted peak characteristic of the  $\nu(\text{SiO}-\text{H})$  modes of the H-bonded silanols, Figure 6. The changes in the  $\nu(\text{SiO}-\text{H})$  region were reversed when the sample was heated to  $80\text{ }^\circ\text{C}$  for 5 h to desorb the less strongly bound H-bonded  $\text{CH}_3\text{ReO}_3$  sites; i.e., the peak assigned to H-bonded silanols disappeared, and the peak due to noninteracting silanols was restored to its initial intensity.

Hydrogen-bonding is also expected to cause a significant downfield shift in the  $^1\text{H}$  MAS NMR signal of the interacting silanol protons.<sup>33</sup> The strongly correlated signal intensity in the 2-D HETCOR spectrum in Figure 3 between the  $^{13}\text{C}$  peak at 20 ppm and the  $^1\text{H}$  peak between 2 and 3 ppm is consistent with this interaction. Unfortunately, the chemical shifts of the signals from H-bonded silanols overlap with those of the methyl protons of grafted  $\text{CH}_3\text{ReO}_3$ . Furthermore, the use of deuterium-labeled  $\text{CD}_3\text{ReO}_3$  to eliminate the signal due to the methyl protons is precluded by extensive H/D exchange between the

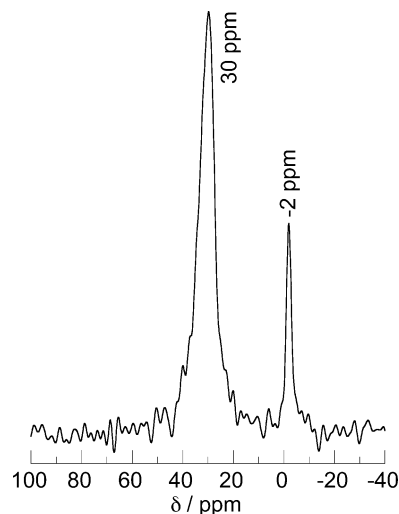
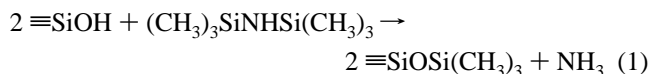


**Figure 7.** Room-temperature  $^{13}\text{C}$  CP-MAS NMR spectrum (12 kHz MAS) of dehydrated silica–alumina modified first with hexamethyldisilazane, followed by  $^{13}\text{CH}_3\text{ReO}_3$  (1 wt % Re).

methyl protons and the surface silanol protons of silica–alumina.<sup>34</sup>

The formation of H-bonded  $\text{CH}_3\text{ReO}_3$  sites on silica–alumina can be prevented by converting the accessible surface silanol groups to siloxanes prior to deposition of  $\text{CH}_3\text{ReO}_3$ . Treatment of dehydrated silica–alumina with an excess of hexamethyldisilazane (HMDS) at room temperature effects this transformation with concomitant generation of ammonia,<sup>35</sup> eq 1:



After reaction, the trimethylsilyl-capped silica–alumina was heated to  $350\text{ }^\circ\text{C}$  under dynamic vacuum to completely desorb  $\text{NH}_3$  from the Lewis acid sites, as judged by the disappearance of the  $\nu(\text{N}-\text{H})$  modes by IR. Deposition of  $^{13}\text{CH}_3\text{ReO}_3$  onto this capped silica–alumina produced a material with two  $^{13}\text{C}$  NMR signals, Figure 7. The peak at  $-2\text{ ppm}$  is assigned to  $(\text{CH}_3)_3\text{Si}$ , while that at  $30\text{ ppm}$  is assigned, as before, to  $\text{CH}_3\text{ReO}_3$  grafted onto Lewis acid sites. No signal at  $20\text{ ppm}$  was observed, consistent with the absence of silanols available to hydrogen-bond to  $\text{CH}_3\text{ReO}_3$ .

A catalyst prepared with trimethylsilyl-capped silica–alumina (0.5 wt % Re) and exposed to the same reaction conditions used to study the activity without hexamethyldisilazane treatment (i.e.,  $0\text{ }^\circ\text{C}$ , 45 Torr of  $\text{C}_3\text{H}_6$ , 10.0 mg of catalyst) behaved similarly toward propene ( $k_{\text{obs}} = 0.13\text{ s}^{-1}$ ). This result indicates that Lewis acidity is both necessary and sufficient for the activation of  $\text{CH}_3\text{ReO}_3$ ; hydroxyl sites are not required. Furthermore, the catalyst prepared with the trimethylsilyl-capped support is a much less active catalyst for olefin isomerization and oligomerization, despite its low Re loading: only propene metathesis products were detected after 60 min of reaction time at  $0\text{ }^\circ\text{C}$ . In contrast, catalysts with low loadings ( $<1\text{ wt \% Re}$ ) that are not trimethylsilyl-capped yield trace amounts of side products such as 1-butene and pentenes under the same reaction conditions.

(32) Herrmann, W. A.; Kühn, F. E.; Roesky, P. W. *J. Organomet. Chem.* **1995**, *485*, 243–251.

(33) Nedelec, J. M.; Hench, L. L. *J. Non-Cryst. Solids* **2000**, *277*, 106–113.

(34) Scott, S.; Moses, A.; Leifeste, H.; Chattopadhyay, S.; Raab, C.; Chmelka, B. F.; Ramsahye, N.; Eckert, J. *Abstracts of Papers*; 229th ACS National Meeting (American Chemical Society), San Diego, CA, 2005; Abstract No. PETR-022.

(35) Rosenthal, D. J.; White, M. G.; Park, G. D. *AIChE J.* **1987**, *33*, 336–340.

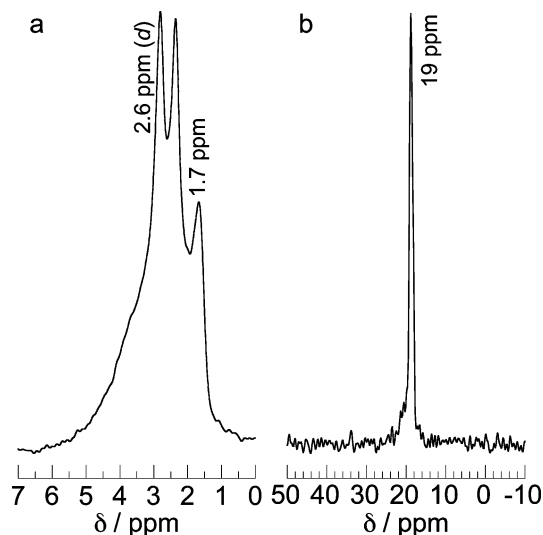


**Figure 8.** Room-temperature solid-state NMR spectra of  $^{13}\text{CH}_3\text{ReO}_3$  adsorbed onto dehydrated silica (recorded after 10 min of exposure to dynamic vacuum, to yield a sample with 4 wt % Re): (a)  $^1\text{H}$  MAS NMR spectrum; (b)  $^{13}\text{C}$  CP-MAS NMR spectrum (12 kHz MAS).

Thus the surface hydroxyl groups are implicated in lowering catalyst selectivity for olefin metathesis. The side reactions can be dramatically slowed either by engaging the hydroxyls in H-bonding interactions with  $\text{CH}_3\text{ReO}_3$  or by trimethylsilyl-capping.

**Deposition of  $\text{CH}_3\text{ReO}_3$  onto Silica.** In order to explore hydrogen-bonding interactions between  $\text{CH}_3\text{ReO}_3$  and surface silanols in the absence of competing adsorption on Lewis acid sites, we deposited  $\text{CH}_3\text{ReO}_3$  onto amorphous silica.  $\text{CH}_3\text{ReO}_3$  does not adsorb strongly on silica and can be completely removed by simple evacuation at room temperature ( $10^{-4}$  Torr). Furthermore,  $\text{CH}_3\text{ReO}_3$  dispersed on amorphous silica (4 wt % Re) shows no activity toward propene self-metathesis under the reaction conditions described above.

The  $^1\text{H}$  MAS and  $^{13}\text{C}$  CP-MAS NMR spectra of  $\text{CH}_3\text{ReO}_3$  dispersed by vapor deposition onto dehydrated silica are shown in Figure 8. A brief (10 min) exposure to dynamic vacuum yielded a material with a loading of 4 wt % Re. Its  $^{13}\text{C}$  CP-MAS spectrum in Figure 8b consists of a single, sharp  $^{13}\text{C}$  peak at 19 ppm (fwhm 1.13 ppm/85 Hz), confirming that  $\text{CH}_3\text{ReO}_3$  is again molecularly dispersed. The chemical shift and line width of the  $^{13}\text{C}$  NMR signal observed for  $\text{CH}_3\text{ReO}_3/\text{SiO}_2$  are remarkably similar to those of the mobile  $\text{CH}_3\text{ReO}_3$  species present at high Re loading on dehydrated silica–alumina. Since silica possesses no Lewis acidity and only weak Brønsted acidity, these results support the assignment of the  $^{13}\text{C}$  NMR signal at 20 ppm for  $\text{CH}_3\text{ReO}_3$  on silica–alumina to mobile species that are hydrogen-bonded to surface silanol groups.

The  $^1\text{H}$  MAS spectrum in Figure 8a contains, in addition to a signal at 1.7 ppm due to unperturbed silanol protons, a doublet attributed to the methyl protons (2.6 ppm,  $^1J_{\text{H-C}} = 135$  Hz) superimposed on a broad signal.<sup>36</sup> The doublet has the same coupling constant as  $^{13}\text{CH}_3\text{ReO}_3$  in  $\text{CDCl}_3$ , and a 2-D  $^{13}\text{C}\{^1\text{H}\}$  HETCOR experiment confirmed that the  $^{13}\text{C}$  signal correlates with the center of the  $^1\text{H}$  doublet (Figure S3). The broad signal centered at ca. 3 ppm is attributed to H-bonded silanols.

(36) The  $^1\text{H}$  signals of grafted  $\text{CH}_3\text{ReO}_3$  are presumably broader on silica–alumina than on silica since  $^1\text{H}$ – $^{13}\text{C}$  coupling was not detected on silica–alumina, even in the  $^1\text{H}$  MAS spectra of  $^{13}\text{C}$ -enriched samples.

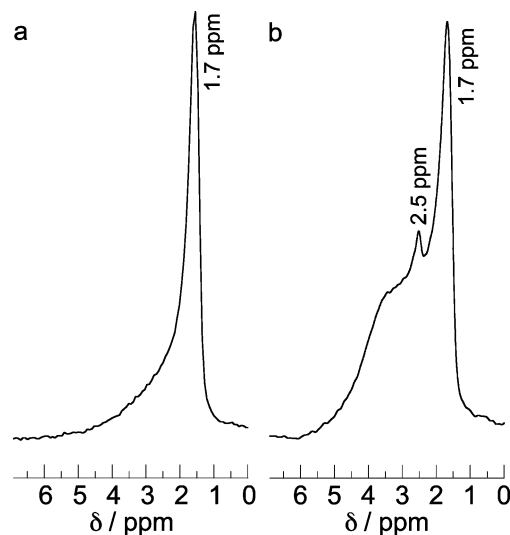


**Figure 9.**  $^1\text{H}$  MAS NMR spectra for (a) dehydrated silica and (b)  $\text{CD}_3\text{-ReO}_3$  (ca. 1 wt % Re) on dehydrated silica, both recorded at room temperature with 12 kHz MAS.

To observe the H-bonded silanols more clearly, the  $^1\text{H}$  MAS NMR spectra of silica before and after adsorption of  $\text{CD}_3\text{ReO}_3$  was recorded, Figure 9. Upon H-bond formation, silanol protons are expected to show broadened, downfield-shifted signals by  $^1\text{H}$  MAS NMR,<sup>37</sup> with the magnitude of the change in chemical shift a function of the strength of the hydrogen bond.<sup>38</sup> Figure 9a shows a sharp signal at 1.7 ppm attributed to noninteracting silanols on silica, with a broad signal at lower field due to the small fraction of silanols that experience H-bonding.<sup>39</sup> In Figure 9b, the presence of  $\text{CD}_3\text{ReO}_3$  results in increased intensity in the broad, downfield signal from 2 to 5 ppm, consistent with H-bonding to the silanols, as well as a small signal for incompletely deuterated methyl groups, at 2.5 ppm. The strong correlation of the  $^{13}\text{C}$  signal for H-bonded  $\text{CH}_3\text{ReO}_3$  at 20 ppm with the broad  $^1\text{H}$  signal at 2.8 ppm in Figure 3 (silica–alumina) and Figure S3 (silica) reflects the dipole–dipole coupling of the methyl carbon with both the methyl protons and the silanol protons in the H-bonded sites. The correlation between the  $^{13}\text{C}$  signal at 28 ppm for  $\text{CH}_3\text{ReO}_3$  engaged in Lewis acid–base bonding to the silica–alumina (Figure 3) is weaker, consistent with dipole–dipole coupling principally between the methyl carbon and the methyl protons.

**Origin of Metathesis Activity.** In summary, four types of materials containing dispersed  $\text{CH}_3\text{ReO}_3$  (0.1–10 wt % Re) have been prepared and characterized, and their metathesis activities compared, for which the spectra and kinetics presented here are representative. One type displays  $^{13}\text{C}$  NMR signals at both 20 and 29 ppm (silica–alumina with >1 wt% Re), two types show only the  $^{13}\text{C}$  signal at ca. 29 ppm (silica–alumina with a  $\leq 1$  wt % Re or capped silica–alumina with up to 6 wt % Re), and one type has only a  $^{13}\text{C}$  signal at 19 ppm (silica). Only materials that display the  $^{13}\text{C}$  CP-MAS peak at 29 ppm are active for propene metathesis. From this result, as well as our structural assignment for these sites, we infer that metathesis activity

(37) Hu, J. Z.; Kwak, J. H.; Herrera, J. E.; Wang, Y.; Peden, C. H. F. *Solid State Nucl. Magn. Reson.* **2005**, *27*, 200–205.

(38) Gardienet, C.; Marica, F.; Fyfe, C. A.; Tekely, P. *J. Chem. Phys.* **2005**, *122*, 054705.

(39) Morrow, B. A. *Stud. Surf. Sci. Catal.* **1990**, *57A*, 161.



correlates with the presence of  $\text{CH}_3\text{ReO}_3$  associated with Lewis acidic Al centers; conversely,  $\text{CH}_3\text{ReO}_3$  that is hydrogen-bonded to hydroxyl groups on either silica or silica–alumina is inactive. This explanation also accounts for the low activating ability of the HY zeolite,<sup>3</sup> which possesses strong Brønsted acid sites but little Lewis acidity. Reports of little or no changes in the structure of  $\text{CH}_3\text{ReO}_3$  upon grafting (as assessed by EXAFS) are likely to be a consequence of preparing materials in which the dominant site is the inactive, H-bonded form of  $\text{CH}_3\text{ReO}_3$ , whose structure is hardly perturbed by this interaction with the support. Furthermore, models for  $\text{CH}_3\text{ReO}_3$  activation based on its proposed condensation with the surface hydroxyls of silica,<sup>6,41</sup> or mechanisms without any organometallic–support interactions,<sup>42</sup> are unable to account for the observed metathesis reactivity. A correlation between metathesis activity and Lewis acidity has been noted for  $\text{CH}_3\text{ReO}_3$  supported on niobia<sup>43</sup> and on Zn-modified aluminas;<sup>40</sup> however, no structures for the grafted sites were proposed.

From this study, it is also clear that the preparation of supported metathesis catalysts with high  $\text{CH}_3\text{ReO}_3$  loadings is an inefficient use of Re, despite the improvement in selectivity. The same effect can be achieved by other methods of blocking the Brønsted acid sites (e.g., by their reaction with hexamethyldi-

silazane). Furthermore, the weaker hydrogen-bonding interactions in the catalytically inactive  $\text{CH}_3\text{ReO}_3$  sites are likely the origin of the severe leaching that has been observed to contaminate metathesis products.<sup>41</sup> The detailed loading dependence of the reaction rate and the mechanism of solid Lewis acid activation of  $\text{CH}_3\text{ReO}_3$  are under investigation.

**Acknowledgment.** This work was funded by the U.S. Department of Energy, Basic Energy Sciences, Catalysis Science Grant No. DE-FG02-03ER15467. The authors thank Marissa Jaffee for Re analysis and Drs. J. D. Epping and J. Hu for helpful discussions. We also thank Dr. Dušanka Janežič and The Center for Molecular Modeling at the National Institute of Chemistry in Ljubljana, Slovenia for use of their computing facility. This work made use of MRL Central Facilities supported by the MRSEC Program of the National Science Foundation, under Award No. DMR05-20415.

**Supporting Information Available:** Complete ref 10; observed and calculated  $^1\text{H}$  and  $^{13}\text{C}$  NMR shieldings and chemical shifts for calibration compounds and models for grafted structures; 2-D  $^{13}\text{C}\{^1\text{H}\}$  HETCOR spectra for  $\text{CH}_3\text{ReO}_3/\text{silica}$ –alumina, recorded at  $-100\text{ }^\circ\text{C}$ , and for  $\text{CH}_3\text{ReO}_3/\text{silica}$ , recorded at room temperature; Cartesian coordinates and calculated energies (in hartrees) for DFT model structures **II**, **III**, and **IV**. This material is available free of charge via the Internet at <http://pubs.acs.org>.

JA072707S

(40) Rost, A. M. J.; Schneider, H.; Zoller, J. P.; Herrmann, W. A.; Kühn, F. E. *J. Organomet. Chem.* **2005**, *690*, 4712–4718.

(41) Zhang, X.; Narancic, S.; Chen, P. *Organometallics* **2005**, *24*, 3040–3042.

(42) Basset, J. M.; Buffon, R.; Choplin, A.; Leconte, M.; Tourode, R.; Herrmann, W. A. *J. Mol. Catal.* **1992**, *72*, L7–L10.

(43) Oikawa, T.; Masui, Y.; Tanaka, T.; Chujo, Y.; Onaka, M. *J. Organomet. Chem.* **2007**, *692*, 554–561.